


New Opportunities for Epicentral Seismic Observations

 **N. K. Kapustian^{a, b}, E. V. Shakhova^a, and G. N. Antonovskaya^{a, *}**
^a *Rykov Federal Center for Integrated Arctic Research, Ural Branch, Russian Academy of Sciences, Arkhangelsk, 163000 Russia*
^b *Schmidt Institute of Physics of the Earth, Russian Academy of Sciences, Moscow, 123242 Russia*
**e-mail: essm.ras@gmail.com*

Received April 5, 2022; revised June 29, 2022; accepted July 5, 2022

Abstract—This study considers the hardware and methodological possibilities for increasing the information content of seismological observations in the epicentral zone of a platform earthquake without obvious surface manifestations. It is shown that the microseismic background analysis conducted during the installation of several seismic stations is efficient for both identifying the source location and refining the geodynamic features of the environment in the epicentral zone. The results of the coherent-time analysis of recordings at the three-component registration made to identify endogenous microcracks hidden by microseismic noise are presented. Their power, number, and azimuths are calculated. The possibility of using an autostructural function for the time series of a stream of micropulses at long-term recording of microseisms is shown to identify the self-organization of crustal blocks by similarities in their geodynamics. The requirements for the seismic equipment necessary for the observations are discussed.

Keywords: three-component registration, frequency band, microseisms, coherence function, time series, auto structural function

DOI: 10.3103/S0747923922060068

INTRODUCTION

One of the main tasks of epicentral observations is to refine the processes in the earthquake source zone, including the role of discontinuous faults. The seismic activity assessment of these faults is an important factor in choosing sites for building critical facilities, for example, high-altitude hydro dams or nuclear power plants. In seismically active regions, this task is solved using a network of seismological stations by analyzing local seismological activities. In platform territories, however, this task is more difficult to solve because their relatively low seismicity and rare seismic networks do not allow making a similar assessment for rarely registered events. In this case, the analysis of microscale earthquakes and microseisms registered by special temporary groups of stations arranged according to the respective regulations is used (Bugayev et al., 2012; *RB-142-18*, 2022).

One of the aspects of the seismic activity assessment of territories is low seismicity analysis (Kayal, 2008; Dyagilev and Shulakov, 2017; Kayal, 2017; Adinolfi et al., 2019; Ma et al., 2021). The significant difference between our approach and the methods of identifying noisy abnormal zones with a network of stationary stations, as for ore mines (Dyagilev and Shulakov, 2017), is as follows: we propose to use records from a small number of sensors, which can be used in epicentral observations for detecting the loca-

tion of a noisy area; in this case, the group can move around the area until it finds the object of interest. The results obtained by this technique are undoubtedly less accurate than the results produced using stationary stations. However, these observations are impossible to conduct in locations without stationary networks.

For example, several works (Rykunov and Smirnov, 1992; Blanter et al., 1997; Narteau et al., 2000) showed that the seismicity hierarchy extends up to endogenous microseisms. Their occurrence is associated with the deformation of a complex block-like geological environment, including displacement of dislocation fault sides (Provost et al., 2018), constrained rotation (Spivak, 1994; Kocharian and Spivak, 2003), and other changes up to deformations caused by lunar-solar tides (Rykunov et al., 1980). It is also essential that the hierarchy of the seismic process extends to the characteristic time of response to straining effects (Kapustian and Yudakhin, 2007), which is important in epicentral zone observations. It should be noted that the leading position in studying this issue is held by researchers from Russia. Thus, the analysis of microseisms registered together with seismic events in the epicentral zone is an additional contribution to understanding the geodynamics involving an earthquake source.

Seismic recordings are processed mainly by isolating events that exceed the background of microseisms.

It takes quite a long time (several months) to obtain statistically reliable estimates. The extraction of microevents hidden by interferences is rare and is done mostly for research purposes (Kocharyan and Spivak, 2003; Kapustian and Yudakhin, 2007; Yudakhin et al., 2008). Nevertheless, it is this method that provides the ability to reduce the observation time and obtain more reliable results based not only on visible weak events but also on microearthquakes and microcracks. When observing weak events and microseisms in an epicentral region, which is sometimes fairly large in area, it is very important to cover it with a network of seismic stations and provide densification of registration points. In the conditions of Russia, these studies are usually very difficult to conduct with one type of equipment. Generally, seismic equipment of various manufacturers is available and can be used for temporary spacings. Difficulties arise during data processing because of the need to consider the frequency response of each sensor, convert the readings to a single format, etc.

This work considers a methodical approach to assessing the seismicity of the investigated area. In this technique, the type and sensitivity of seismic equipment are not critical because statistical parameters and dimensionless characteristics of microseisms are evaluated. The goal of the study was to justify the requirements on the recording equipment and develop a data processing technique for more efficient seismometric surveys.

The basis of this approach was formed during the survey of faults in the Arkhangelsk oblast' (Yudakhin et al., 2005), as well as on the Solovetsky Islands while studying the nature of microfractures at an external environment, that is, the deforming impact on a full-scale model of a boulder dike (Yudakhin et al., 2008). It is significant that the work was carried out using different recorders (with 16- to 32-bit processors). However, this had practically no effect on the quality of the results. It was shown that the dislocation faults were strain-sensitive structures and responded to small changes in external load (by less than 0.1 bar) by changing the power of microevent streams. In addition, an algorithm for processing three-component (X , Y , Z) seismic records by calculating coherence functions in pairs for recording components X – Y , X – Z , and Y – Z was developed. A more detailed description of the algorithm is given below. It was also proven that the sensitivity region of the technique extended to 20 km in size (Yudakhin et al., 2008).

Despite the fact that the technique was developed more than 15 years ago, it has not been widely used, apparently due to its absence in the survey regulations. Now, this technique is used in the Verov Federal Center for Integrated Arctic Research, Ural Branch of the Russian Academy of Sciences (FECIAR UrB RAS) for studying various objects (tectonic knots, kimberlite pipes, etc.). The technique was called the method of

microseism activity (MMA). This method will be used hereafter and is part of the set of passive seismic observation methods. It should be noted that unlike other similar methods designed to investigate the structure of the crust this technique is so far the only passive method that allows characterizing the geodynamics of objects.

This paper discusses the requirements for observational equipment and shows the capabilities of the MMA based on the example of studying the epicentral zone of the Kholmogory earthquake that occurred on March 28, 2013 in the north of the East European Platform (EEP).

MATERIALS AND METHODS

Summary for Geological and Geophysical Data on the Epicentral Site

According to the tectonic scheme (Baluev et al., 2012), the zone, in which the Baltic Shield joins with the northwestern margin of the Russian Plate, is represented by the movable White Sea belt. This possibility is confirmed by seismological studies of the influence of spreading on the seismicity of the northern EEP (Antonovskaya et al., 2021). In addition to such factors as the discharge of partial stresses generated by lithospheric plates, postglacial glaciation unloading, and induced seismicity, the seismicity of the EEP is influenced by the joint activities of mid-oceanic ridges. In particular, the time and place of the earthquake that occurred on March 28, 2013 can stem from disturbances due to the spreading from Mohns and Gakkel Arctic ridges, which are a type of trigger for stress removal. The epicenter of the earthquake was approximately 1800–2500 km from the rifts. According to the simulation results (Antonovskaya et al., 2021), the maximum disturbance at distances of about 2000–2500 km is 6–10% of the disturbance applied to the rift. The earthquake occurred at the time when the Mohns and Gakkel ridges exhibited high coefficients of the correlation of the annual seismic energy curves for these ridges and the platform; thus, the maximum disturbances from the ridges during their mutual influence may reach 12–20%. It is quite possible that the combination of disturbances was the trigger for the prepared earthquake.

According to an analysis of the refined epicenters of the earthquakes that occurred in the north of European Russia from 1542 to 2019 (Nikonov, 2013; Morozov et al., 2020), the northwest of the region was shaken by violent earthquakes with a magnitude up to 6 at depths of 20–25 km, whereas the earthquakes that occurred in the rest of the territory had a magnitude no higher than 4. The Kholmogory earthquake of March 28, 2013 ($t_0 = 07:02:16.5$, 63.97° N, 41.5° E, $h = 21$ km, $M_L = 3.4$) was confined to the same seismogenic zone as the event of October 22, 2005 ($t_0 =$

17:46:44.8, 64.49° N, 40.95° E, $h = 13$ km, $M_L = 2.9$) (Morozov et al., 2016; Morozov et al., 2020).

When investigating the possibility of new seismic events, it is necessary to analyze the seismotectonic situation that already exists in the northwestern region. The Arkhangelsk ledge is a kind of “wedge” embedded into the fracture in the modern Kandalaksha graben (Zykov et al., 2008). The main mechanism of the movements is discharge.

Figure 1 shows a diagram of the seismic studies of the epicentral zone located in the contour of the so-called Kholmogory tectonic junction (Kutinov et al., 2020). We used the data of the regional seismic surveys (see Fig. 1): the GSS profile (“Agat-5”) (Egorkin, 1996) and DOM (I-I) (Ermolaeva, 2002); together with the results of studies by microseism sounding method (MSM), the seismic survey data allow definition of the structural-geological situation near the epicenter of the 2013 earthquake. Structural studies show that the epicenter zone of the Kholmogory earthquake shows in seismic fields as crustal lamination disturbances and manifestations of vertical structures in the crustal tops.

Equipment and Observation Plan

The observations by MAM were conducted using a stationary cross-like arrangement of four broadband seismic sensors that encompassed a potential earthquake source; three stations were located at the epicentral zone boundary. According to the calculations by FECIAR UrB RAS, the boundary was situated about 15 km away from the epicenter (Morozov et al., 2020), whereas the northern point was situated about 20 km away from the epicenter. We note that this spacing of points is characteristic of works aimed at choosing an NPP site.

Three-component Canadian-made Nanometrics TC-120s seismometers with Centaur recorders were used as the recording equipment. The horizontal components were oriented along the cardinal directions (N–S, E–W). A significant feature of the sensors is that they were broadband: if the chosen survey frequency was 100 Hz, it was possible to make recordings in the sub-50 Hz band. According to our experience, it is this band that is characterized by the main streams of informative microcracks. It was planned to conduct the observations for about 3 weeks, which was more than enough to accumulate the necessary statistical material (Yudakhin et al., 2005, 2008; Kapustian and Yudakhin, 2007). Unfortunately, all of the stations worked simultaneously only the first 7 days and the last 3 days. This was due to the fact that the stations were powered from regular car batteries, which were periodically replaced. It was impossible to calculate their operating time for each station for timely replacement. An alternative used for similar works by FECIAR UrB RAS is batteries of higher capacitance

or solar batteries. However, the latter are effective only in protected places, for example, near railroads.

Sensors should be arranged considering the “noisiness” of the point, including technogenically induced noisiness. In our case, the influence of the M8 highway had an impact. As a result, records made at night and morning hours were accepted for processing: 00:00 to 06:00 according to local time. To make the processing more convenient, the continuous records were divided into two 3-hour intervals, that is, files of 00:00 to 03:00 and 03:00 to 06:00.

Method of Microseism Activity

Unlike structural passive methods using surface waves (Shapiro et al., 2005; Draganov et al., 2009; Gorbatikov et al., 2013; Afonin et al., 2017), the microseismic activity method is based on the bulk waves emitted by the source in the medium thickness. Surface sources are rejected by comparing the results for different sections, namely in horizontal plane X – Y and in vertical planes X – Z and Y – Z .

Considering that there is no single interpretation of the microevent concept in the literature, let us explain the object of this study by summarizing the experience in observations (Spungin et al., 1997; Kapustian, 2001; Yudakhin et al., 2005; Dyagilev and Shulakov, 2017). In this study, the terms “microevent,” “microrattle,” or “micropulse,” are understood as natural endogenous (not technogenic) waveforms present on a seismic record as short wavetrains or wavetrains extended in time. As a rule, a microevent exceeds the background, while microcracks and micropulses are disturbances at or below the background level. All these oscillations are represented mainly by bulk waves. Examples of the first and the second case (microevents exceeding or comparable to the background) are shown in Fig. 2.

Type one microevents are characterized by higher intensity and lower frequency than type two events. The spectra can be judged by spectral-time charts at frequencies above 10 Hz (Fig. 3). Lower frequencies that manifest high power are represented by near-surface noises.

The MMA is based on calculating coherence function k_{ij} for components (i, j) in pairs (Yudakhin et al., 2005, 2008) as

$$k_{ij}(f) = \frac{|S_{ij}(f)|}{\sqrt{S_{ii}(f)S_{jj}(f)}}, \quad (1)$$

where $S_{ii}(f)$, $S_{jj}(f)$ are the power spectra of each of the microseismic components; $S_{ij}(f)$ is the averaged mutual spectrum of component pairs. If the medium has no separate radiation sources and microseisms are represented by white noise evenly collected from all of the directions, then $k_{ij} = 0$. If there is a source of vibrations in a certain direction, $0 < k_{ij} \leq 1$ is the frequency

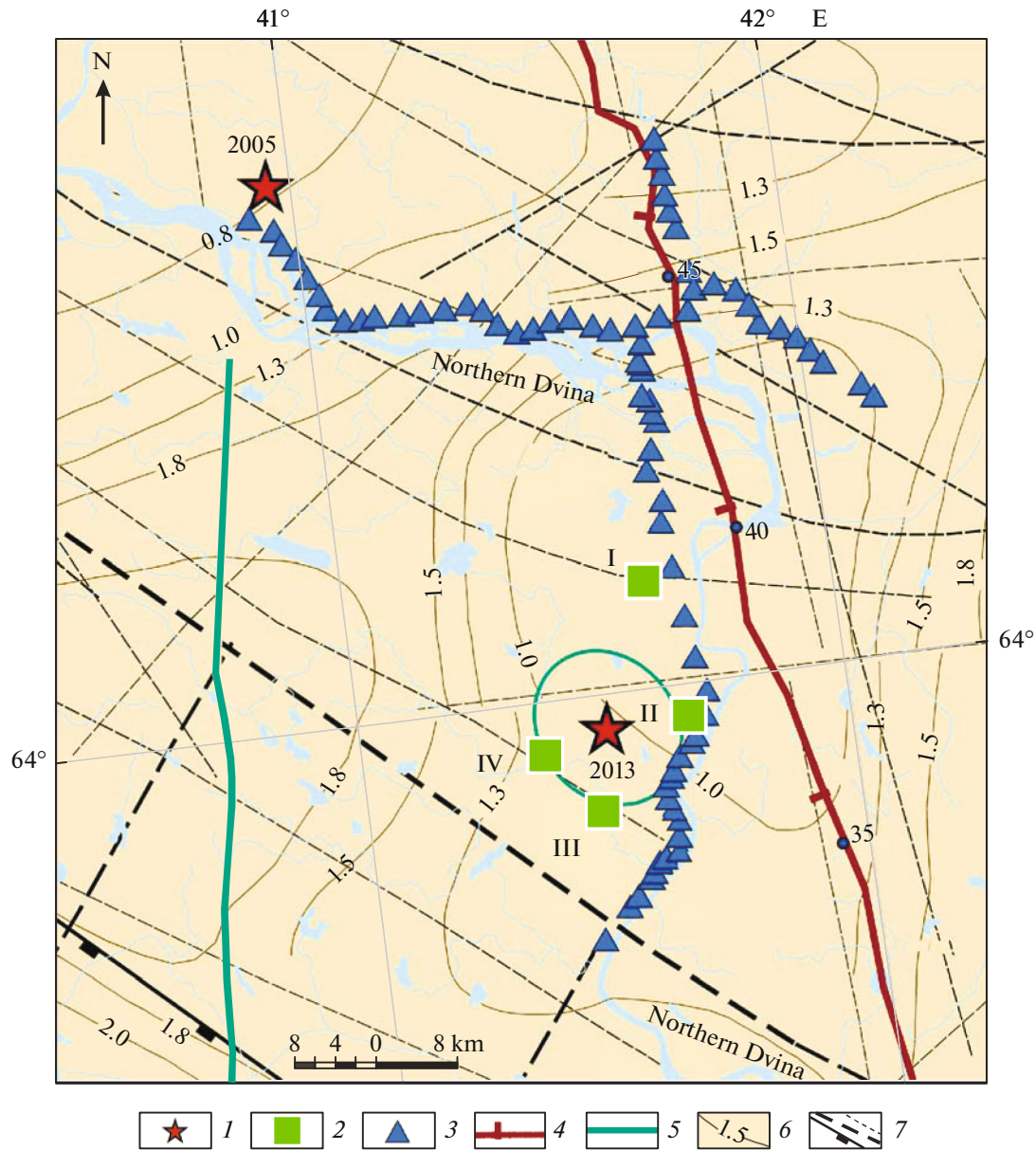


Fig. 1. The layout of the seismic tests and tectonic violations in the region of the Kholmogory earthquake in 2013: 1 is the epicenters of the earthquakes taken place on October 22, 2005 and March 28, 2013; 2 is the temporary network of seismic observations; 3 is the microseism measurement profiles; 4 is the Agat DSS profile (Egorkin, 1996); 5 is the profile of CMP CDP I-I (Ermolaeva, 2002); 6 is the foundation contour lines; 7 is discontinuous faults of different grades.

band of this source. The greater the signal/interference ratio is, the higher the value of the coherence $k_{ij}(f)$ is (equality to one corresponds to the complete absence of interferences). The analysis of the coherence function values for component pairs $X-Z$ and $Y-Z$ allows estimating the vertical sections of the medium (latitudinal or longitudinal) to which the signal source is closer. In this sense, MMA can be likened to a “seismic radar.”

Usually, especially while estimating the seismic activity of dislocation faults, we deal with a set of sources from some radiating zone in a sufficiently broad range of frequencies and not with a single source. In this case, experience shows that it is necessary to consider the entire frequency band of endogenous radiation (Yudakhin et al., 2008). The processing procedure is confined to calculating component power spectra (spectral-time analysis abbreviated as

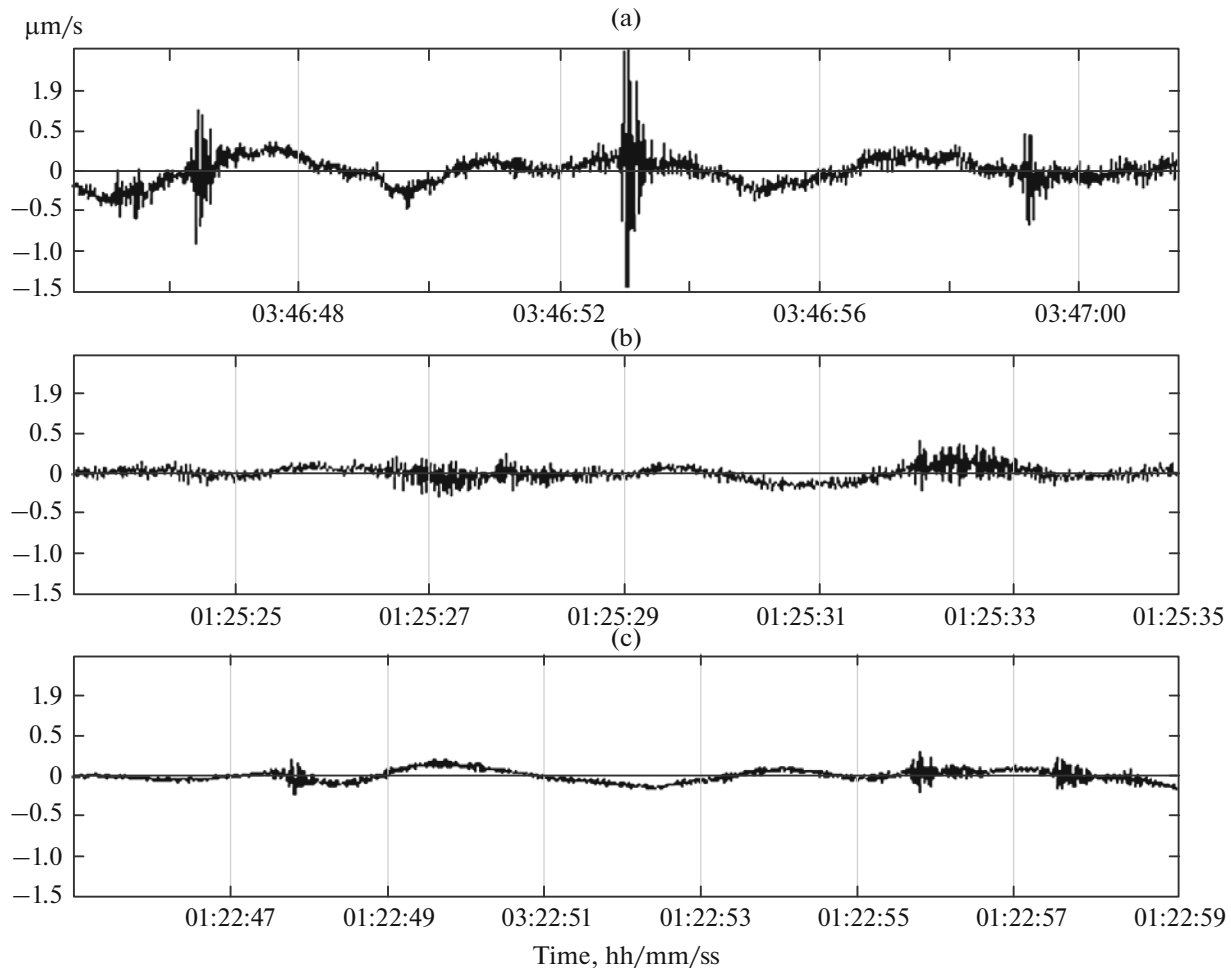


Fig. 2. The waveforms of microevents for vertical channel Z: (a) are microevents exceeding the background by capacity; (b) and (c) are microevents comparable with the background by capacity.

STAN) and coherence functions (coherence-time analysis known abbreviated as CTAN).

Examples of STAN and CTAN for our case are shown in Fig. 3. The comparison of STAN and CTAN diagrams emphasizes the advantage of using the coherence function for detecting weak seismic radiation from a local area against the background of the record noisy with a number of natural and anthropogenic interferences. As well, this comparison allows an understanding of which frequency range should be chosen; in our case, the chosen frequency range is the 20–40 Hz band, where the strongest radiation is observed.

It is known that the noise signal for volumetric waves consists from a mixture of *P*- and *S*-waves. In terms of intensity, their ratio depends on the type of noisy inhomogeneity. Depending on the type of waves that are prevalent in terms of power, the respective direction to the source will be determinative. To assess the reality of the identified direction to the source, geological and geophysical interpretation is con-

ducted, first of all, with reference to geological structural features, such as dislocation faults. In addition, data on different points of simultaneous micropulse measurements are compared. It is essential that the MMA is designed for tests at a radial distance of up to 20 km from the sensor (Yudakhin et al., 2008); remote sources are not identified, which is conditioned by the high-frequency range.

SURVEY RESULTS

In the first processing phase, events exceeding the microseismic background were identified by looking through the records. Those events were single but their number per hour ($\langle n \rangle$) was different for different observation points (Table 1). The highest and the lowest number of microevents was recorded, respectively, at observations points IV and II.

In the next processing phase, CTAN diagrams were plotted for all of the recordings round-the-clock. The total distributions of k_{ij} values for each CTAN diagram

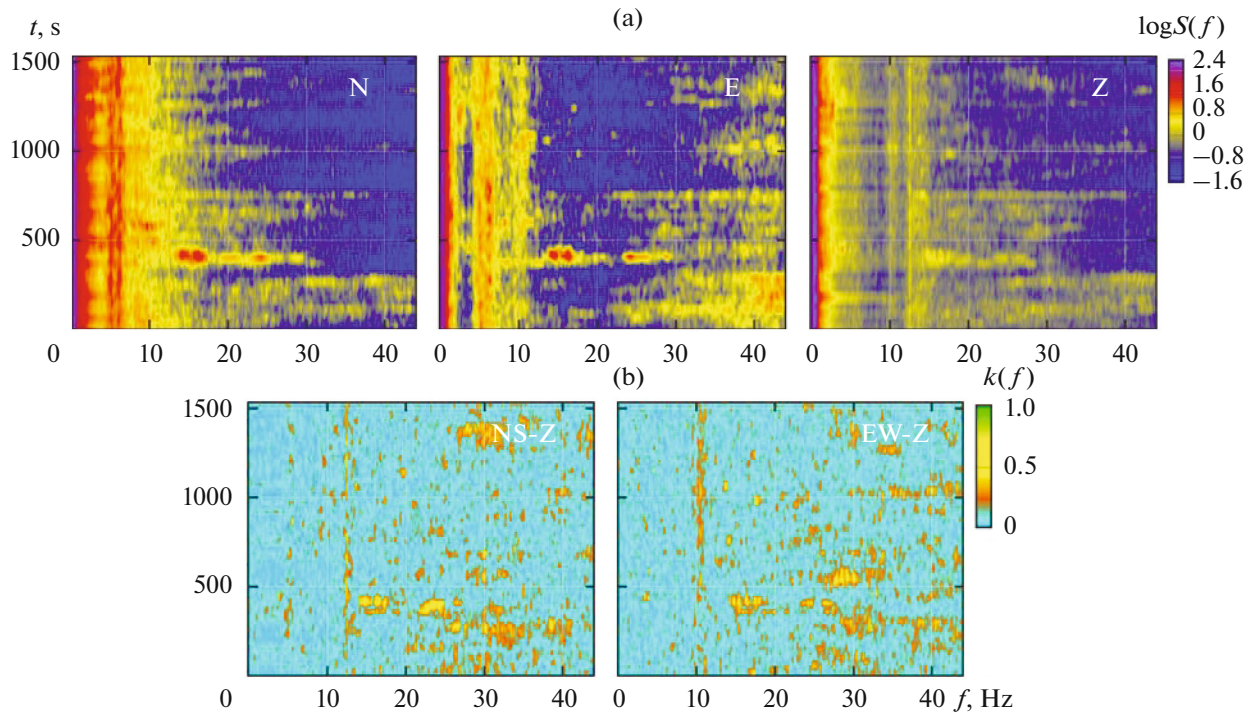


Fig. 3. Examples of (a) STAN diagrams and (b) CTAN diagrams for observation point IV (see Fig. 1).

in longitudinal section (NS–Z) and latitudinal section EW–Z were calculated in the 20–40 Hz frequency band. An example of the distribution for all of the days for point IV is given in Fig. 4a. The obtained distributions are similar to those for the Zipf law for the properties of complex structured environments or its special case, the Gutenberg–Richter relation in seismology (Gutenberg and Richter, 1944; Zipf, 1949; Merriam et al., 2004). Previously, we showed the possibility of considering the k_{ij} quantity, defined as the ratio of signal/interference intensities, as an energy characteristic of the stream of microfrequencies (Yudakhin et al., 2008).

Viewing the distributions for different points shows their similarity in shape; however, the mutual location of the curves is different: the curve for NS–Z can be higher than the curve for EW–Z and vice versa. Furthermore, to be able to compare the data, we will consider the $N_{0.6}$ quantity defined as the number of events

at $k_{ij} = 0.6$, i.e., when the signal is already more powerful than the interference and the number of events is sufficient for further statistical analysis. The diagram of the values of parameter $N_{0.6}$ for different points in sections NS–Z and EW–Z is shown in Fig. 4b. There is a significant difference in the directivity of seismic radiation in the following points: at pt. I, the sources are located mainly in the longitudinal section; at pt. II, they are located mainly in the latitudinal section. This agrees with the main direction of development of the modern geodynamic situation of the region (Zykov et al., 2008).

Distributions of k_{ij} , for which arrays $\{N_{0.6}\}$ were determined, followed by the calculation of the parameters of descriptive statistics, were constructed for each interval, for all of the days and points. The statistical estimates for sections NS–Z and EW–Z, calculated for the dataset for night hours only on each of the first 7 days of the observations, are shown in Table 1. The

Table 1. The parameters of seismic radiation in the NS–Z and EW–Z cross-sections. See clarification in the main text

Point	NS–Z		EW–Z		Azimuth, deg	R^2	$\langle n \rangle$
	$\langle N_{0.6} \rangle$	$\sigma N_{0.6}, \%$	$\langle N_{0.6} \rangle$	$\sigma N_{0.6}, \%$			
I	610	13	148	13	16	0.77	2–3
II	101	21	253	26	87	0.04	1–2
III	125	41	82	19	22	0.62	4
IV	275	13	118	24	45	0.62	7

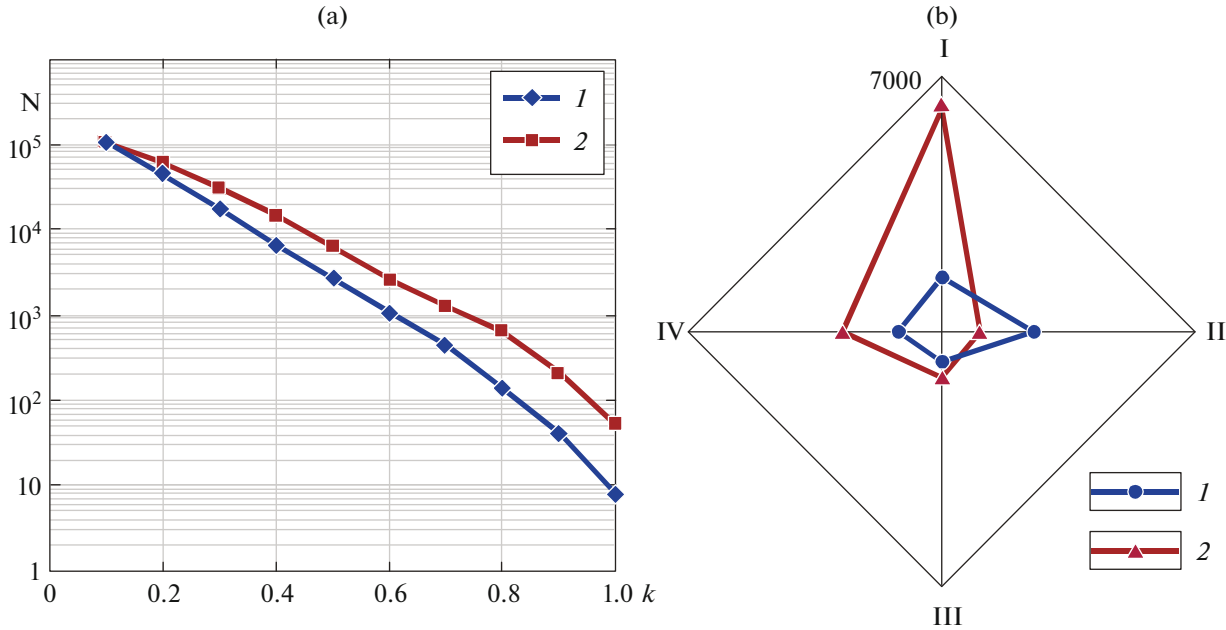


Fig. 4. The parameters of microseismic radiations along directions EW–Z (1) and NS–Z (2) for the entire period of observations: (a) is the distribution of the coherent function for point IV; (b) is the diagram of the number of events at $k = 0.6$.

estimates are the median value $\langle N_{0.6} \rangle$, standard deviation, azimuth defined as the linear trend of the NS–Z...EW–Z scatter diagram, the value of reliable approximation of this linear trend R^2 , and $\langle n \rangle$, which is the number of visually distinguished microevents.

DISCUSSION

In addition to the above-mentioned difference in the overall directivity of seismic radiation at different points, let us note the values of R^2 at these points. The largest value of this quantity corresponds to the proximity of the azimuths of the sources on different days to the average azimuth, while the small values indicate a large scatter of points relative to the selected direction, i.e., a rather chaotic arrangement of the sources. The first case is seen at pt. I; the second case is seen at pt. II. This agrees with the idea that the microevent sources at pt. I are confined to the fault structure identified by structural studies (the DSS profile (“Agat-5”) (Egorkin, 1996), CDP (I-I) (Ermolaeva, 2002) and MSM). For the situation at pt. II, the concept of the properties of microseismic radiation in a fractured block medium is suitable. In this medium, events occur at the boundaries of blocks and everything depends on their position relative to each other and on the external stress field. For example, a case of this kind is described by the model of constrained rotation (Kocharyan and Spivak, 2003). Strong fragmentation is also evidenced by a small number of relatively strong (visually distinguishable) events in this point (see Table 1).

Let us demonstrate another possibility for interpreting the materials during long-range three-component broadband observations. We refer to the comparison of the time course of estimates at different points. This comparison allows, e.g., combining points into cluster regions with identical properties in the case of similarities in time change curves or establishing a sequence of processes in different zones. Unfortunately, the issue with the power supply of the stations does not allow one to conduct this study in a full manner due to omissions and nonuniformity of the data in time.

Nevertheless, in this case, the autostructural function (ASF) $C(T)$ defined as the mathematical expectation

$$C(T) = M [N(t) - N(t + T)]^2 \tag{2}$$

can be used for time series $N(t)$ represented by a random function with stationary increment.

As shown in (Kanamori et al., 1979), the ASF shape reflects differences in the dynamics of processes: the position of the first local maximum of $C(T)$ on axis T corresponds to the period of quasi-sinusoidal pulses (wavetrains), contained in time series $N(t)$, whereas the position of the first absolute maximum corresponds to the relative duration of these pulses.

If $N(t)$ contains random nondeterministic components, the ASF is approximated by function $C(T) = T^\alpha$, and there is a linear trend at $\alpha \geq 2$. If the curve asymptotically tends to “saturation” and is characterized by saturation time T_{st} , then the $C(T_{st})/T_{st}$ ratio

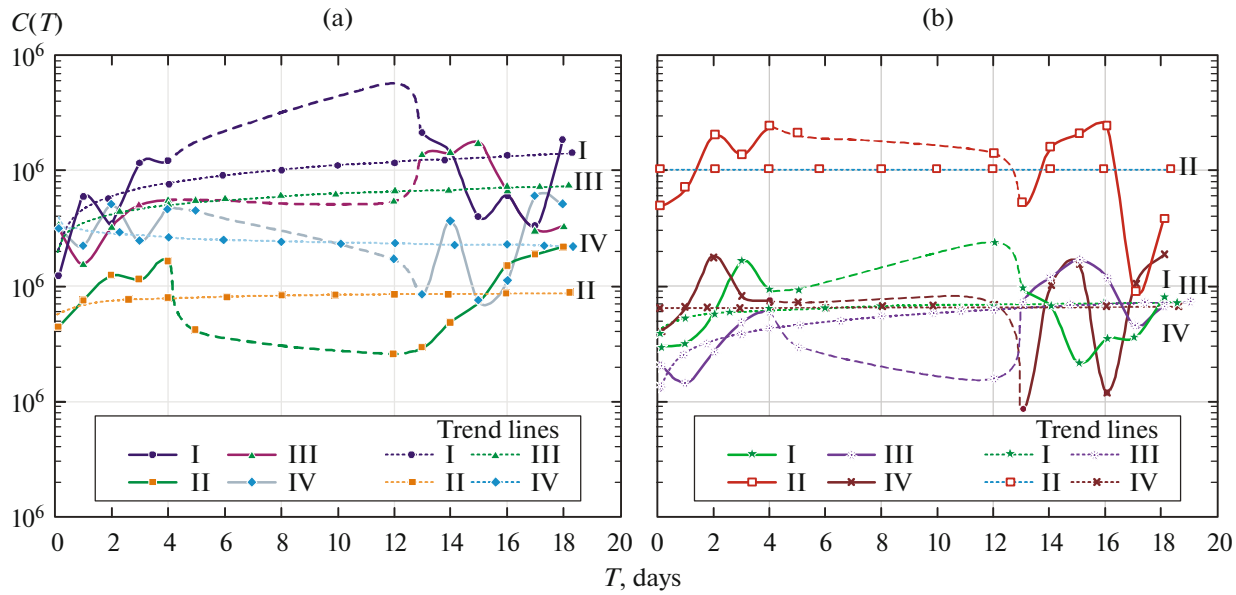


Fig. 5. The autostructural functions of time variations $N_{0,6}(t)$ along directions NS–Z (a) and EW–Z (b) for observation points I–IV.

indicates the average rate of change in parameters for noncyclic processes.

Figure 5 shows the ASF values of $N_{0,6}(t)$ in the longitudinal and latitudinal sections for all of the observation points. The first points of the curves correspond to $T = 3$ h; the dotted line shows the course of the curves in time intervals with insufficient statistics. The position of the first maximum and the absence of curve trends ($\alpha < 1$) are reliably determined for all of the plots.

The time interval that corresponds to the first maximum and characterizes the periodicity in seismic emission is different for different observation points (Table 2): for pt. I for longitudinal wavetrains (NS–Z) the period is 1 day, and for latitudinal wavetrains (EW–Z) along the regional fault (see Fig. 1) this period is 3 days. The periods for pt. II and IV are 2 days for both, the points and directions. However, no wavetrains are distinguished for pt. III.

According to the MSM profiles (see Fig. 1), the presence of vertical disturbances in the south of the epicenter zone was confirmed (Danilov, 2017). The earthquake source is located in the middle crust and

the displacement plane is subvertical, extending approximately in the longitudinal direction.

One of the possible explanations of these results is described below. Outside the epicentral zone (point I), the microseismic radiation generated by the regional fault is oriented predominantly transversely to it, which can stem not from displacements along the fault but from subvertical displacements.

This is also indicated by the periodicity of single-day radiation wavetrains, which may be related to lunar–solar tides (Rykunov et al., 1980). Points II, III, and IV at the edges of the epicentral ellipse have similar radiation characteristics that differ, however, from those at point I. Points II and IV follow the same rhythm, which indicates the commonality of their geodynamics, but are opposite in radiation direction (see Fig. 4). Point III is quite passive. All of this, as well as the rotation of the radiation azimuth between points II and III, suggests the possibility of constricted rotation mechanisms for the epicentral zone. We note that the epicentral ellipse was derived only by processing the data on the 2013 earthquake. Thus, not only was the position of the earthquake epicenter confirmed but also the reliability of the seismological data with their processing by the FECIAR UrB RAS.

Let us discuss the requirements for the seismic recording equipment. According to our experience, the level of endogenous microseisms recorded on the diurnal surface in the 10–50 Hz frequency band exhibits significant variations in different regions, but lies in the $1 \times 10^{-3} - 1$ ($\mu\text{m/s}^2/\text{Hz}$) power range (Kapustian and Yudakhin, 2007). Considering that the processing analyzes the statistics of the microseismic recording power rather than the features of each

Table 2. The parameters of autostructural functions

Point	NS–Z		EW–Z	
	T_1 , ds	α	T_1 , ds	α
I	1	0.4	3	0.1
II	2	0.2	2	0
III	–	0.1	–	0.3
IV	2	0.1	2	0

microcracking waveform, any modern seismological sensor, including popular domestic seismometers SM3-KV, will work for such studies. The main characteristics of SM3-KV are a frequency range of 0.5–50 Hz, sensitivity of 120–170 V/(m/s), and dynamic range of 96 dB. The work (Chebrov et al., 2013) provided the characteristic frequency and amplitude ranges of signals read by seismometers of different types, which can be successfully used for analyzing microseismic activities.

Similarly, any modern device with a 24-bit ADC capacity can be used as a recorder; however, recorders with low-bit processors will also work (the sufficient condition for suitability is an ADC capacity of 16-bit).

CONCLUSIONS

This work has shown that the endogenous microseismic background can be used in analyzing the epicentral zone of platform earthquakes. The utilization of these data provides new opportunities for geological environment surveys. The most essential of these opportunities are:

- division of the epicentral zone in regions with different seismic activities and different deformation evolution periods;

- refinement of the position of the epicenter, which is especially important for platform earthquakes, where the source is usually covered with a thick sedimentary layer (for example, in our case, its thickness is 1–2 km).

It is essential that the analysis of microseisms made proceeding from the hierarchy of the seismic process and considering estimates of the parameters of the recurrence schedule allows a significant reduction in the observation time (for example, to a period from 2 weeks to 1 month). The actual observation interval is determined on the basis of the specific local conditions of a surveyed territory (the noisiness of the observation point, logistics of the works, etc.). This is especially important for platform territories, where violent earthquakes are rare.

The requirements for making observations and selecting recording equipment with sufficient interpreting capabilities are:

- (1) When selecting seismic sensors, it is necessary to pay attention to their sensitivity, which should not be lower than 120 V/(m/s), and dynamic range, which should not be lower than 96 dB. An example of the equipment suitable for such studies is Russian SM3-KV seismometers.

- (2) Seismometers should have at least three components (a vertical and two horizontal channels), oriented either along the cardinal sections or along and across geological structures. If it is necessary to specify the azimuth of the radiating zone, for example, along the rhumbs or the fault zone, several single-component sensors can be used, for example, one vertical and

more than two horizontal CM-3KV gages. The observations can be supplemented with the recording of torsional vibrations.

- (3) Data should be recorded into built-in memory. Recorders with low-bit processors (at least 16 bits) are acceptable.

- (4) When arranging autonomous stations, it is important to ensure their uninterrupted power supply, which will allow analysis of long-term series of observations. In this case, either solar batteries or sufficiently high-capacity batteries can be installed on the condition of their periodic replacement. For example, when TS-120s sensors with Centaur recorders (made by Nanometrics) are used, which consume approximately 1.5 W in total, a 24 V 70 Ah LiFePO₄ lithium-iron-phosphate battery will ensure 2 months of uninterrupted power supply for one temporary seismic station, which is generally a sufficient time window for the seismic activity assessment of a fault zone by the microseismic activity method.

We hope that the foregoing considerations will make it possible to substantially enrich seismic epicentral observations and use the entire spectrum of available equipment.

FUNDING

The work was written as part of state task 122011300389-8 of the Federal Center for Integrated Arctic Research of the Ural Branch of the Russian Academy of Sciences State Registration and state task FMWU-2022-0020 of the Schmidt Institute of Physics of the Earth of the Russian Academy of Sciences.

CONFLICT OF INTEREST

The authors declare that they have no conflicts of interest.

REFERENCES

- Adinolfi, G.M., Cesca, S., Picozzi, M., Heimann, S., and Zollo, A., Detection of weak seismic sequences based on arrival time coherence and empiric network detectability: An application at a near fault observatory, *Geophys. J. Int.*, 2019, vol. 218, no. 3, pp. 2054–2065. <https://doi.org/10.1093/gji/ggz248>
- Afonin, N., Kozlovskaya, E., and Kukkonen, I., and DAFNE/FINLAND working group, Structure of the Suasselkä postglacial fault in northern Finland obtained by analysis of local events and ambient seismic noise, *Solid Earth*, 2017, vol. 8, no. 2, pp. 531–544. <https://doi.org/10.5194/se-8-531-2017>
- Antonovskaya, G.N., Basakina, I.M., Vaganova, N.V., Kapustian, N.K., Konechnaya, Y.V., and Morozov, A.N., Spatiotemporal relationship between arctic mid-ocean ridge system and intraplate seismicity of the European Arctic, *Seismol. Res. Lett.*, 2021, vol. 92, no. 5, pp. 2876–2890. <https://doi.org/10.1785/0220210024>

- Baluev, A.S., Zhuravlev, V.A., Terekhov, E.N., and Przhivalgovskii, E.S., *Tektonika Belogo morya i prilegayushchikh territorii* (Tectonics of the White Sea and Adjacent Territories), Leonov, M.G., Ed., Moscow: GEOS, 2012.
- Blanter, E.M., Shnirman, M.G., Le Mouél, J.L., and Allegre, C.J., Scaling laws in blocks dynamics and dynamic self-organized criticality, *Phys. Earth Planet. Inter.*, 1997, vol. 99, nos. 3–4, pp. 295–307.
[https://doi.org/10.1016/S0031-9201\(96\)03195-0](https://doi.org/10.1016/S0031-9201(96)03195-0)
- Bugaev, E.G., Kishkina, S.B., and Sanina, I.A., Seismic monitoring peculiarity of atomic energy facilities at East European Platform, *Yadern. Radiats. Bezop.*, 2012, no. 3, pp. 3–11.
- Chebrov, V.N., Droznin, D.V., Kugaenko, Yu.A., Levina, V.I., Senyukov, S.L., Sergeev, V.A., Shevchenko, Yu.V., and Yashchuk, V.V., The system of detailed seismological observations in Kamchatka in 2011, *J. Volcanol. Seismol.*, 2013, vol. 7, no. 1, pp. 16–36.
<https://doi.org/10.1134/S0742046313010028>
- Danilov, K.B., The structure of the Onega downthrown block and adjacent geological objects according to the microseismic sounding method, *Pure Appl. Geophys.*, 2017, vol. 174, pp. 2663–2676.
<https://doi.org/10.1007/s00024-017-1542-x>
- Draganov, D., Campman, X., Thorbecke, J., Verdel, A., and Wapenaar, K., Reflection images from ambient seismic noise, *Geophysics*, 2009, vol. 74, no. 5, pp. A63–A67.
<https://doi.org/10.1190/1.3193529>
- Dyagilev, R.A. and Shulakov, D.Yu., Location of noise-like signals sources with local seismic networks, *Sovremennye metody obrabotki i interpretatsii seismologicheskikh dannykh* (Modern Methods of Processing and Interpretation of Seismological Data), Obninsk, Kaluga oblast: Edinaya Geofiz. Sluzhba Ross. Akad. Nauk, 2017, pp. 155–158.
- Egorin, A.V., Multi-wave deep seismic studies, *Geofizika*, 1996, no. 4, pp. 25–30.
- Ermolaeva, G.M., *Informatsionnyi otchet o rezul'tatakh rabot po teme: Seismorazvedochnye raboty. Mezenskaya sinekliza (profil' I–I)* (Information Report on Results of Work in the Topic: Seismic Exploration Studies: Mezenskaya Syncline (Profile I–I), Arkhangelsk: Arkhangel'skii TGF, 2002.
- Gorbatikov, A.V., Montesinos, F.G., Arnoso, J., Stepanova, M.Yu., Benavent, M., and Tsukanov, A.A., New features in the subsurface structure model of El Hierro Island (Canaries) from low-frequency microseismic sounding: An insight into the 2011 seismo-volcanic crisis, *Surv. Geophys.*, 2013, vol. 34, no. 4, pp. 463–489.
<https://doi.org/10.1007/s10712-013-9240-4>
- Gutenberg, B. and Richter, R.F., Frequency of earthquakes in California, *Bull. Seismol. Soc. Am.*, 1944, vol. 34, pp. 185–188.
<https://doi.org/10.1785/BSSA0340040185>
- Kanamori, K., F'yuz, G., and Nevskii, M.V., Temporal variations of residuals in travel time of R-wave on stations of Southern California by the data of quarry explosions, *Sb. sovetско-amerikanskikh rabot po prognozu zemletryaseni* (Collection of Soviet-American Works on Prediction of Earthquakes), Dushanbe: Donish, 1979, vol. 2, book 1, pp. 81–94.
- Kapustyan, N.K., Seismic activation of lithosphere in far zone of earthquakes and tectonic sources, *Sovremennaya geodinamika, glubinnoe stroenie i seismichnost' platformnykh territorii i sopredel'nykh raionov. Materialy mezhdunarodnoi konferentsii* (Recent Geodynamics, Deep Structure, and Seismicity of Platform Territories and Adjacent Regions), Voronezh: Voronezh. Gos. Univ., 2001, pp. 89–91.
- Kapustian, N.K. and Yudakhin, F.N., *Seismicheskie issledovaniya tekhnogennykh vozdeistvii na zemnyu koru i ikh posledstviu* (Seismic Studies of Technogenic Impacts on the Earth's Crust and Their Consequences), Yekaterinburg: Ural. Otd. Ross. Akad. Nauk, 2007.
- Kayal, J.R., *Microearthquake Seismology and Seismotectonics of South Asia*, Dordrecht: Springer, 2008.
<https://doi.org/10.1007/978-1-4020-8180-4>
- Kayal, J.R., Hydraulic fracturing and microseismicity: Global perspective in oil exploration, *Georesursy*, 2017, vol. 19, no. 3, pp. 222–228.
<https://doi.org/10.18599/grs.19.3.12>
- Kocharyan, G.G. and Spivak, A.A., *Dinamika deformirovaniya blochnykh massivov gornykh porod* (Deformation Dynamics of Block Massifs of Rocks), Moscow: Akademkniga, 2003.
- Kutinov, Yu.G., Chistova, Z.B., and Neverov, N.A., New data on the impact of tectonic nodes on the state of the environment at the north of the Russian plate, *Vestn. Mosk. Univ. Ser. 5, Geogr.*, 2020, no. 5, pp. 12–24.
- Ma, T., Tang, C., Liu, F., Zhang, S., and Feng, Z., Microseismic monitoring, analysis and early warning of rockburst, *Geomatics, Nat. Hazards Risk*, 2021, vol. 12, no. 1, pp. 2956–2983.
<https://doi.org/10.1080/19475705.2021.1968961>
- Merriam, D.F., Drew, L.J., and Schuenemeyer, J.H., Zipf's law: A viable geological paradigm?, *Nat Resour. Res.*, 2004, vol. 13, pp. 265–271.
<https://doi.org/10.1007/s11053-004-0134-5>
- Morozov, A.N., Vaganova, N.V., and Konechnaya, Ya.V., Tectonic earthquakes of October 22, 2005 and March 28, 2013 in the north of the Russian plate, *Izv., Phys. Solid Earth*, 2016, vol. 52, no. 4, pp. 520–533.
<https://doi.org/10.1134/S1069351316030095>
- Morozov, A.N., Vaganova, N.V., Konechnaya, Y.V., Zueva, I.A., Asming, V.E., Noskova, N.N., Sharov, N.V., Assinovskaya, B.A., Panas, N.N., and Evtyugina, Z.A., Recent seismicity in northern European Russia, *J. Seismol.*, 2020, vol. 24, no. 1, pp. 37–53.
<https://doi.org/10.1007/s10950-019-09883-6>
- Narteau, C., Shebalin, P., Holschneider, M., Le Mouél, J.-L., and Allègre, C.J., Direct simulations of the stress redistribution in the scaling organization of fracture tectonics (soft) model, *Geophys. J. Int.*, 2000, vol. 141, no. 1, pp. 115–135.
<https://doi.org/10.1046/j.1365-246X.2000.00063.x>
- Nikonov, A.A., A new stage in understanding seismicity of the East European Platform and its margins, *Dokl. Earth Sci.*, 2013, vol. 450, part 2, pp. 638–642.
<https://doi.org/10.1134/S1028334X13060032>
- Provost, F., Malet, J.-P., Gance, J., Helmstetter, A., and Doubré, C., Automatic approach for increasing the location accuracy of slow-moving landslide endogenous seismicity: The APOLoc method, *Geophys. J. Int.*, 2018, vol. 215, no. 2, pp. 1455–1473.
<https://doi.org/10.1093/gji/ggy330>

RB-142-18: Guide in safety in using nuclear energy: Seismological monitoring of areas of placing nuclear and radiation-dangerous objects, 2018. <https://docs.cntd.ru/document/551819875>. Cited March 15, 2022.

Rykunov, L.N. and Smirnov, V.B., Seismology of micro scale, *Vulkanol. Seismol.*, 1992, no. 3, pp. 3–15.

Rykunov, L.N., Khavroshkin, O.B., and Tsyplakov, V.V., Moon-Sun tidal periodicity in spectral lines of temporal variations of high-frequency microseisms, *Dokl. Akad. Nauk SSSR*, 1980, vol. 252, no. 3, pp. 577–580.

Shapiro, N., Campillo, M., Stehly, L., and Ritzwoller, M., High-resolution surface-wave tomography from ambient seismic noise, *Science*, 2005, vol. 307, pp. 1615–1618. <https://doi.org/10.1126/science.1108339>

Spivak, A.A., Relaxation control and dynamics of massifs of rocks, *FTPRPI*, 1994, no. 5, pp. 8–26.

Spungin, V.G., Dubinya, V.A., and Ivanchenko, G.N., Experimental diagnostics of structure and geodynamics of massifs of rocks based on analysis of microseismic oscillations, *Vulkanol. Seismol.*, 1997, no. 6, pp. 42–50.

Yudakhin, F.N., Kapustian, N.K., Antonovskaya, G.N., and Shakhova, E.V., Detection of weakly active faults of platforms using nanoseismic technology, *Dokl. Akad. Nauk*, 2005, vol. 402, no. 4, pp. 533–538.

Yudakhin, F.N., Kapustian, N.K., and Shakhova, E.V., *Issledovaniya aktivnosti platformennykh territorii s ispol'zovaniem microseism* (Studies of Activity of Territories Using Microseisms), Yekaterinburg: Ural. Otd. Ross. Akad. Nauk, 2008.

Zipf, G.K., *Human Behavior and the Principle of Least Effort: An Introduction to Human Ecology*, Addison-Wesley Press, 1949.

Zykov, D.S., Kolodyazhnyi, S.Yu., and Baluev, A.S., Signs of horizontal movements of basement in White Sea region, *Byull. Mosk. O-va Ispytatelei Prir. Otd. Geol.*, 2008, vol. 83, no. 2, pp. 15–25.

Translated by S. Kuznetsov